Available online at www.sciencedirect.com

ScienceDirect

Geochimica et Cosmochimica Acta 236 (2018) 336–350

Geochimica et Cosmochimica Acta

www.elsevier.com/locate/gca

Lithium isotopic composition of benthic foraminifera: A new proxy for paleo-pH reconstruction

J. Roberts [a,*], K. Kaczmarek [a], G. Langer [c], L.C. Skinner [b], J. Bijma [a], H. Bradbury [b], A.V. Turchyn [b], F. Lamy [a], S. Misra [b,d,*]

[a] *Alfred-Wegener-Institut Helmholtz-Zentrum für Polar- und Meeresforschung, 27570 Bremerhaven, Germany*
[b] *The Godwin Laboratory for Paleoclimate Research, Department of Earth Sciences, University of Cambridge, UK*
[c] *The Marine Biological Association of the United Kingdom, The Laboratory, Citadel Hill, Plymouth, Devon PL1 2PB, UK*
[d] *Centre for Earth Sciences, Indian Institute of Science, Bangalore, India*

Received 2 October 2017; accepted in revised form 23 February 2018; available online 13 March 2018

Abstract

The lithium isotopic composition of foraminifera is an established tracer of long-term changes in the global silicate weathering cycle, following the assumption that foraminifera faithfully record the lithium isotopic composition (δ^7Li) of seawater. In this study, we demonstrate by utilising benthic foraminifera (*Amphistegina lessonii)* that were cultured under decoupled pH-[CO_3^{2-}] conditions, that foraminifera δ^7Li is strongly dependent on pH. This is reinforced with δ^7Li data from globally distributed core-top samples of *Cibicidoides mundulus* and *Cibicidoides wuellerstorfi*, which show the same negative correlation with pH. The dependency of δ^7Li on pH is perhaps a surprising result given that lithium speciation in seawater is independent of both pH and carbonate ion speciation. The dependence of lithium incorporation on growth rate was assessed by measuring the calcium isotopic composition; no growth rate dependent incorporation was observed. Instead, we propose that the strength of the ^{6}Li and ^{7}Li hydration spheres (and hence their respective desolvation energy) is pH-dependent, resulting in a significant isotopic fractionation during the incorporation of lithium into foraminifer calcite. The core-top derived δ^7Li-pH calibration is used to demonstrate the applicability of this δ^{11}B-independent pH proxy in reconstructing deglacial variations in pH in the South Pacific. The use of foraminifera δ^7Li to compliment δ^{11}B-based pH reconstructions has the potential to provide insight into time-dependent variations in porewater/seawater δ^{11}B, temperature and salinity, which were previously unresolvable.

Keywords: Lithium isotopes; Culture; Core-top; pH

1. INTRODUCTION

Lithium is a conservative cation in seawater. The long residence time of lithium in seawater (~1.2 Myr) relative to the mixing time of the ocean (~1000 years) means that modern seawater is homogenous with respect to lithium concentration (26 μM) and isotopic composition (δ^7Li = 31.0 ± 0.5‰) (Millot et al., 2004). Over millions of years, continental and seafloor silicate weathering and the reverse weathering (clay formation) cycle has led to significant changes in the ocean δ^7Li, which is recorded in planktonic foraminifera (Hathorne and James, 2006; Misra and Froelich, 2012). The core-top calibration of planktonic foraminifera conducted by these studies revealed that most

* Corresponding authors at: Centre for Earth Sciences, Indian Institute of Science, Bangalore, India (S. Misra); Alfred-Wegener-Institut Helmholtz-Zentrum für Polar- und Meeresforschung, 27570 Bremerhaven, Germany (J. Roberts).
E-mail address: sambuddha@iisc.ac.in (S. Misra).

https://doi.org/10.1016/j.gca.2018.02.038
0016-7037/

species recorded δ^7Li values similar to seawater. This led to the assumption that foraminifera faithfully record secular changes in seawater δ^7Li.

More recently, this idea was challenged by the culture study of Vigier et al. (2015), which demonstrated that the δ^7Li of benthic foraminifera *Amphistegina lobifera* is a function of the dissolved inorganic carbon (DIC) concentration in seawater. These new findings suggest that foraminifera δ^7Li could be dominantly controlled by local environmental conditions and thus both expands the possible application of foraminifera δ^7Li as paleoceanographic proxy whilst limiting the use of foraminifera δ^7Li in reconstructing chemical weathering fluxes in the geological past. However, to-date, the Vigier et al. (2015) study is the only one of its kind to show an environmental control on foraminifera δ^7Li. Moreover, as the authors suggest that the lithium isotope fractionation response to changes in the concentration of DIC in foraminifera is related to the mechanism of biomineralisation, it remains to be seen whether all species of foraminifera respond in a similar manner.

In this study, we start with a similar study to Vigier et al. (2015), investigating the effect of changes in pH and DIC on the δ^7Li of *Amphistegina lessonii*. Furthermore, we utilise the foraminifer calcite δ^{44}Ca to investigate the relationship between rate of calcite precipitation and lithium incorporation (Li/Ca). Unlike Vigier et al. (2015) we do not find a significant response of *Amphistegina* δ^7Li to DIC, but instead observe a strong negative correlation between δ^7Li and pH. We use globally distributed core-top samples of *Cibicidoides mundulus* and *Cibicidoides wuellerstorfi* to demonstrate that the trends observed in the culture experiment are reproduced in the modern ocean. Finally, we apply our new δ^7Li-pH proxy to a downcore record, to quantify the deglacial changes in pH in the deep South Pacific, and make a comparison between δ^7Li and δ^{11}B-derived pH.

2. MATERIAL

This study is comprised of three parts: (i) a culture study of the benthic foraminifera *Amphistegina lessonii* under decoupled carbonate chemistry, (ii) a global core-top study of two species of benthic foraminifera, *Cibicidoides mundulus* and *Cibicidoides wuellerstorfi*, and (iii) a lithium isotope record from the deep South Pacific measured on *Cibicidoides mundulus*. We discuss here the material used in each of these three sections before detailing the lithium and boron isotope methodology.

2.1. Culture study

Details of the culture study are elucidated in Kaczmarek et al. (2015), however we reiterate the key points here. *Amphistegina lessonii* were cultured from juveniles under decoupled pH-[CO_3^{2-}] conditions as summarised in Table 1. The advantage of this decoupled carbonate chemistry setup is that it allows us to uniquely determine the primary driver, i.e. pH or [CO_3^{2-}], behind trace element and isotopic responses – unlike core-top calibration studies where pH and [CO_3^{2-}] are positively correlated. The seawater culture was altered by bubbling it with 180 ppm CO_2 or by adding stock solutions of $NaHCO_3$ and Na_2CO_3 in specific ratios as needed to be in equilibrium with given pCO_2. Seawater was further modified by adding $B(OH)_3$ to achieve a final $[B]_{Matrix}$ 10 times greater than natural seawater. In order to keep the carbonate system constant during foraminifer growth, the culture media was replaced every third day. Regular measurements of pH, DIC, TA and CO_2(g) confirm the stability of the carbonate system during culture. The 2σ error based on replicate measurements of the culture matrix was 0.1 pH units, 20 μmol/kg and 40 μmol/kg for pH, DIC and TA, respectively. The [CO_3^{2-}] was calculated from pH and DIC, giving a 2σ error of 20 μmol/kg. The δ^7Li and δ^{11}B of both the cultured foraminifera and the culture matrix (from before and after the experiment) were determined, and show no evidence of contaminant lithium from preparation of the culture matrix (Fig. S1). Since juveniles were grown under different ratios of pH-to-[CO_3^{2-}] immediately after they were spawned, the initial calcite weight was negligible compared to the final weight of the harvested adults.

It should be noted that the experiments by Kaczmarek et al. (2015) were designed to decouple pH from [CO_3^{2-}] and *vice versa* and not to create constant DIC conditions. However, two treatments resulted in DIC concentrations of around 2000 μmol/kg (2093 and 2261 μmol/kg, on average 2177 μmol/kg), referred to as ca. 2000 μmol/kg hereafter, and another two treatments have a DIC concentration around 4000 μmol/kg (3890 and 4128 μmol/kg, on average 4009 μmol/kg), referred to as ca. 4000 μmol/kg hereafter.

2.2. Core-top study

Late Holocene samples were taken from 14 cores spanning 598 m–3710 m depth in the Atlantic and South Pacific (Fig. 1; Table S2). Core material was washed and sieved >63 μm with deionised water. Two species of epi-benthic foraminifera (*Cibicidoides wuellerstorfi* and *Cibicidoides mundulus*) were picked for trace element and isotope analysis (images of the foraminifera analysed in this study are shown in the Supporting Information, Fig. S8).

Radiocarbon dating of planktonic foraminifera from select surface samples reveal ages of >1000 years (Table S1). Based on these dates, we assume that the core-top benthic foraminifera from these sites are Pre-Industrial in age. Therefore, to compare the isotopic composition of these foraminifera with contemporaneous carbonate chemistry, we derived pre-industrial DIC by subtracting anthropogenic CO_2 from DIC in the GLODAP gridded dataset (Key et al., 2004) for the effect of anthropogenic CO_2 input (Sabine et al., 2004). The calculated pre-industrial DIC was used in combination with the GLODAP alkalinity dataset (Key et al., 2004) and annual temperatures and salinities derived from the World Ocean Database 2013 (Boyer et al., 2013), to derive ocean carbonate chemistry using the R package "seacarb". The uncertainty in the temperature and salinity was determined by taking the standard deviation of the seasonal gridded data for each core location. The uncertainty in carbonate chemistry was taken from the reported uncertainties in DIC and

Table 1
Carbonate chemistry summary of treatments used in Kaczmarek et al. (2015). Detailed information about the carbonate system for each treatment is given in the supplementary material of Kaczmarek et al. (2015).

Treatment	pH (2σ)	$[CO_3^{2-}]$ (μmol/kg) (2σ)	$[DIC^{-}]$ (μmol/kg) (2σ)
A	8.1 ± 0.1	160 ± 20	1257 ± 20
B	8.6 ± 0.1	640 ± 20	2261 ± 20
C	8.1 ± 0.1	640 ± 20	5736 ± 20
D	8.1 ± 0.1	540 ± 20	4128 ± 20
E	7.9 ± 0.1	260 ± 20	3890 ± 20
F	8.1 ± 0.1	260 ± 20	2093 ± 20

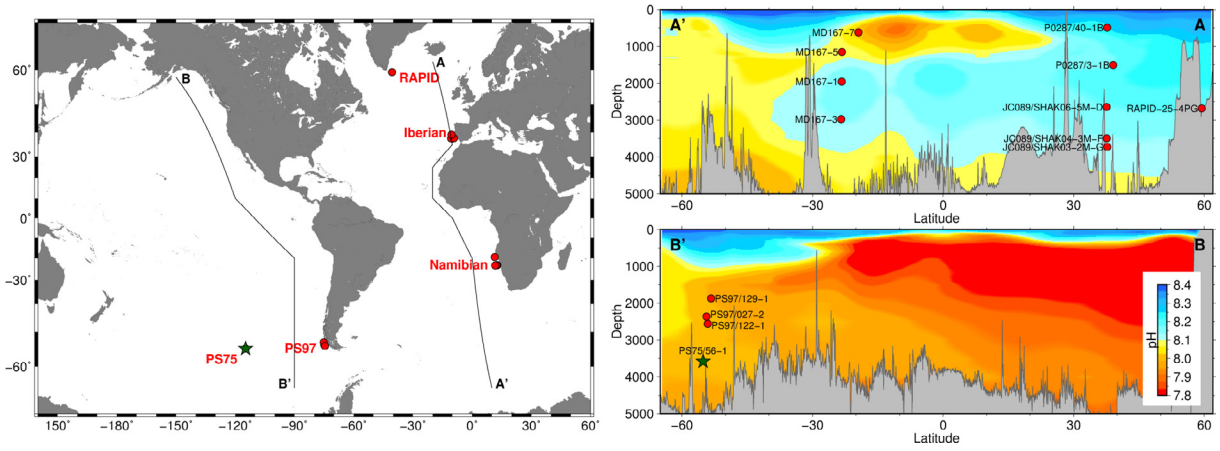

Fig. 1. Map and pre-industrial pH transects of the Atlantic and Pacific showing the location of cores used in this study. (Left) Map of surface samples (red points) and the downcore site (green star) used in this study. (Top right panel) Pre-industrial pH transect of the Atlantic, along line A-A′ shown on the map. All the Atlantic cores have been projected onto this section. (Bottom right panel) Pre-industrial pH transect of the Pacific, along line B-B′ shown on the map. All the Pacific cores have been projected onto this section. (For interpretation of the references to colour in this figure legend, the reader is referred to the web version of this article.)

alkalinity in the GLODAP gridded dataset. Note that pH is expressed on the total scale throughout. We emphasise that there is a large uncertainty in the site-specific inferred carbonate chemistry primarily resulting from (i) the interpolation of the spatially non-uniform GLODAP database, and (ii) the anthropogenic carbon correction. An additional source of error is the observable in the porewater pH and $[CO_3^{2-}]$ profiles of core sites underneath regions of strong upwelling (e.g. the Namibian margin). Large pH gradients exist in the top 10 cm of the sediment (Fontanier et al., 2013), primarily driven by the oxidation of organic matter. Should the foraminifer reside within the top few cm of sediment (rather than at the surface) – as has been observed in the case of *C. mundulus* [e.g. Gottschalk et al., 2016] – they could record carbonate chemistry that is significantly different to bottom water conditions.

2.3. Down-core record

Specimens of *Cibicidoides mundulus* (100–300 μg) were picked from the gravity core PS75/056-1 from the deep South Pacific (55°09.74′S; 114°47.31′W; 3581 m water depth; Fig. 1, star). The core is located on the eastern flank of East Pacific Rise about 300 km north of the Sub-Antarctic Front.

The age model (Ullermann et al., 2016) for the core was based on the correlation of the benthic $\delta^{18}O$ record to the LR04 benthic $\delta^{18}O$ stack (Lisiecki and Raymo, 2005). We acknowledge that the age model is relatively poorly constrained, but for the purposes of this study, where the focus is on the comparison between boron and lithium isotopes, it is sufficient.

3. METHODS

3.1. Foraminifera preparation

All foraminifera specimens were chemically processed and analysed as described below, apart from $\delta^{11}B$ of the culture samples which were determined by laser ablation as detailed in Kaczmarek et al., (2015). The culture matrix was also analysed for lithium and boron isotopic composition following chemical separation and mass spectrometry identical to that used for foraminifera samples.

Foraminifera samples were prepared for $\delta^{11}B$ analysis following Misra et al. (2014a). Briefly, each foraminifer was cracked open and the clays removed following Barker et al. (2003). After transferring samples to a new vial, samples were reductively cleaned using an ammonia-ammonium acetate buffer and hydrazine to remove ferro-manganese coatings. Samples were then oxidatively cleaned using a sodium hydroxide buffer and hydrogen peroxide to remove organics (Boyle and Keigwin, 1985; Rosenthal et al., 1997; Barker et al., 2003). Following the chemical

cleaning, samples were leached in very dilute (0.001 M), double-distilled HCl to release any chemically adsorbed elements from the calcite surface. The leached samples were dissolved in 80 µl of double-distilled 0.7 N HCl and centrifuged. The supernatant 72 µl was used for $\delta^{11}B$ analysis. The remaining 8 µl was diluted with 200 µl of 0.1 N HNO_3 and used for trace element analysis.

3.2. Trace element analysis

Trace element analysis was conducted following Misra et al. (2014a). Briefly, 50 µl of the 208 µl trace element cut was diluted 5-fold in 0.1 N HNO_3 and analysed via ICP-OES to determine [Ca] (de Villiers et al., 2002). The concentration of minor elements (e.g. B/Ca and Li/Ca) were subsequently determined at 10 ppm Ca using a Thermo® Element XR by diluting the trace element aliquot using 0.1 N HNO_3 + 0.3 M HF solution. Samples were analysed in blocks of seven with a pair of acid blanks and internal consistency standards bracketing each block.

The concentrations of foraminiferal trace elements of interest (Li, B, Mg, Al, Sr, Cd, Ba and U) were measured at a fixed detection model to avoid detection mode switch during analysis. Calcium was measured in both low and medium resolution to maintain accuracy of each elemental ratio obtained from the two mass resolution modes. The 2σ for each elemental ratio was determined based on replicate measurements of an internal foraminifera standard (CAM-wuell) and is reported in the supporting information (Table S3).

3.3. Boron isotopic composition

Boron was separated from the calcite matrix using a micro-distillation technique (Gaillardet et al., 2001; Wang et al., 2010; Misra et al., 2014b), which utilises the volatile nature of boric acid. The residue from the micro-distillation process was kept for δ^7Li analysis.

Boron isotopic ratios were analysed by Thermo® Neptune Plus® MC-ICP-MS (fitted with Jet interface) at the University of Cambridge following concentration matched Standard-Sample bracketing technique at 5 or 10 ppb [B] depending on sample size. NIST 951a was used as the bracketing standard. All samples and standards were diluted in 0.5 M HF and analysed in wet plasma conditions (RF = 1350 W, 50 µl/min aspiration rate) utilising a Savillex® Teflon® single pass Scott type spray chamber. Jet sampling and 'X' skimmer cones were utilised to boost sensitivity. Both isotopes were measured on E^{13} Ω amplifiers (Lloyd et al., 2018) at ~100 mV (for 5 ppb [B]) or ~200 mV (for 10 ppb [B]) beam size for ^{11}B. Procedural blanks were <1 mV for ^{11}B, i.e. ≤10 pg. Secondary reference material AE-121 ($\delta^{11}B = 19.9 \pm 0.6$‰, Vogl and Rosner, 2012) was analysed every fifth sample to calculate within run precision. A seawater sample and two duplicate *C. mundulus* samples, which had all undergone micro-distillation purification, were analysed during each analytical session (Fig. S2). Their 2σ error spread over multiple instrument session was 0.40‰, 0.23‰ and 0.67‰ for the seawater sample, first and second *C. mundulus* samples respectively. The upper-limit of 0.67‰ was reported as the procedural 2σ error, and used throughout the manuscript.

The *in-situ* pH was derived from *C. mundulus* $\delta^{11}B$ using the following equation:

$$pH = pK_B^* - \log\left(-\frac{\delta^{11}B_{sw} - \delta^{11}B_{CaCO_3}}{\delta^{11}B_{sw} - \alpha_B.\delta^{11}B_{CaCO_3} - 1000(\alpha_B - 1)}\right) \quad (1)$$

We assume that foraminiferal $\delta^{11}B$ is equivalent to $\delta^{11}B_{borate}$ of the growth matrix (Rae et al., 2011), α_B = 1.0272 (Klochko et al., 2006), $\delta^{11}B_{sw}$ = 39.61 ‰ (Foster et al., 2010) and $B_T = 432.5 \times (S/35)$ µmol/kg (Lee et al., 2010). This choice of constants has been demonstrated to provide faithful estimates of pH using core-top *Cibicidoides* in the Atlantic (Rae et al., 2011). Note that in this calculation, World Ocean Database 2013 (Boyer et al., 2013) annual temperatures and salinities are used, as *in-situ* temperature and salinity measurements are not available.

3.4. Lithium isotopic composition

The residue from the micro-distillation post boron purification contains all the non-volatile matrix elements including lithium. This residue was re-dissolved in 150 µl of calibrated double-distilled 0.7 N HCl. The separation of lithium from its matrix follows ion exchange chromatography outlined in Bohlin et al. (2018). Briefly, samples were loaded in 150 µl of 0.7 N HCl onto high aspect ratio 1.5 ml columns (3.2 mm ID and 20 cm long) containing macroporous sulphonyl cation exchange resin AGMP-50 (BioRad™) (Strelow, 1984; Strelow, 1989). The columns were then eluted with 4 ml of 0.7 N HCl (pre-Li cut), with the first 1 ml added incrementally to ensure the sample was quantitatively loaded onto the resin. Lithium was then eluted in 0.7N HCl and collected as a 6.5 ml cut. A 0.5 ml pre- and post-Li cut was collected to ensure there was no sodium interference and that all the lithium was contained in the 6.5 ml cut. Following column elution the lithium fraction was dried down at 90 °C before being refluxed for 24 h with concentrated double distilled HNO_3. This converts the sample to a nitrate salt and oxidises any organic matter derived from possible resin degradation. The refluxed samples were dried down and were then taken up in 2% HNO_3 for δ^7Li analysis. Seawater samples (culture matrix) were first dried down, refluxed with concentrated double-distilled HNO_3, taken up in calibrated 0.7 N HCl, and ca. 0.5 ng of lithium then processed through columns.

High precision δ^7Li analysis was performed at the University of Cambridge on the Thermo® Neptune Plus® MC-ICP-MS (fitted with Jet interface). The instrument is operated in dry plasma conditions (1200 W) utilising ESI™ APEX-IR. A concentration matched standard-sample bracketing technique was used to correct for instrumental drift and mass bias. Both isotopes of lithium were determined on E^{13} Ω amplifiers (Bohlin et al., 2018). Utilising a 100 µl/min nebulizer, Jet sampling and 'X' skimmer cone a lithium sensitivity of 1 V per ppb was routinely achieved. Samples were analysed at [Li] of 0.2 ppb (0.1 ng-Li per analysis), producing a beam of 90

mV and 6 mV on the ^{7}Li and ^{6}Li detector. Procedural blank was <2 mV and <0.3 mV on the ^{7}Li and ^{6}Li detector, equating to 1–3 pg Li, i.e. ≤1% of the smallest sample. For a few samples with ≤100 pg of lithium, it was not possible to achieve the required concentration of lithium, samples with a <25% concentration mismatch to the standard were corrected (as described in the Supporting Material) and the remaining samples were rejected from this analysis. Each standard and sample was followed by a background instrumental blank measurement in 2% HNO_3 matrix, enabling interpolated blank correction. Lithium isotopic ratios were determined with respect to NIST L-SVEC standard (Flesch et al., 1973). We use an external ^{7}Li enriched secondary reference standard ($\delta^{7}Li = 30.2‰$) and column-processed the extremely low concentration lithium aragonitic coral NEP (0.05–0.15 ng Li per sample) to monitor long-term accuracy and precision of the analytical method. The average values of secondary reference material analysed at [Li] of 0.2 ppb (0.1 ng-Li per analysis) was 30.93 ± 0.91‰ (n = 45) and the column processed coral standard (NEP) was 17.11 ± 0.84‰ (2σ; n = 8) (0.2 ± 0.1 ng of Li per sample). The 2σ error reported for each data point is based on duplicate measurements of the same sample. Low mass samples which were not analysed in duplicates (in particular, a few of the downcore samples), the 2σ values reported are based on analysis of multiple column-processed NEP coral.

3.5. Calcium isotopic composition

Chemically cleaned cultured *A. lessonii* were dissolved and an aliquot containing ca. 6 μg Ca, in solution, was separated. This Ca fraction was spiked with a 1:10 ratio of $^{42}Ca/^{48}Ca$ double spike and then refluxed with double-distilled concentrated HNO_3. Following spike equilibration, the sample was dried down and re-dissolved in 0.5% HNO_3 and calcium was separated utilising a Thermo Scientific™ DIONEX™ ICS 5000+ in cation exchange mode. Eluted calcium samples were dried down, refluxed with concentrated double-distilled HNO_3, dried and loaded on to Rhenium filaments. Calcium isotope ratios ($\delta^{44}Ca$) were determined by a Thermo Scientific™ TRITON *Plus*™ at the University of Cambridge following the method outlined in Fantle and DePaolo, 2005 . All $\delta^{44}Ca$ values are reported on the Bulk Silicate Earth (BSE) scale. A minimum of five replicates of NIST 915b (SRM) were co-processed with every batch of samples and analysed on the Thermo Scientific Triton Plus Thermal Ionisation Mass spectrometer (TIMS). The samples were analysed on the TIMS at ~10 V of ^{40}Ca beam on a 10^{11} Ω resistor with a minimum of 200 cycles per measurement. The long-term analytical uncertainty (2σ) on chemically processed NIST 915b was 0.1‰.

3.6. Linear regression

Given that a large fraction of the data plotted here has error in both the x and y component, we have determined each linear regression using a weighted total least squares optimisation, using the R package Deming. The R^2 value and p-value have been used to determine the significance of each correlation.

4. RESULTS

4.1. Culture study

The cultured *A. lessonii* reveal a striking negative correlation between the lithium isotopic composition of the foraminifer shell ($\delta^{7}Li_{SHELL}$) and the pH of the culture matrix (Figs. 2a and 3a). However, at constant pH, there is no significant correlation between $\delta^{7}Li_{SHELL}$ and DIC (Figs. 2b and 3b), or $\delta^{7}Li_{SHELL}$ and $[CO_3^{2-}]$ (Fig. 3c).

There is no discernible trend between Li/Ca ratio of *A. lessonii* and pH (Fig. 3d). However, there is a positive correlation ($R^2 = 0.55$, $p = 0.08$) between the Li/Ca ratio and DIC concentration (Fig. 3e), but no correlation between Li/Ca and $[CO_3^{2-}]$ (Fig. 3f).

The calcium isotopic composition ($\delta^{44}Ca$) of inorganic calcite is linked to the kinetics of mineral precipitation (Tang et al., 2008; DePaolo, 2011). In foraminifera, the $\delta^{44}Ca$ appears to respond to both rates of precipitation and temperature (Nägler et al., 2000; Gussone et al., 2003; Hippler et al., 2006; Kisakürek et al., 2011). Since temperature was held constant in our culture experiments, we use the $\delta^{44}Ca$ as a first order proxy for the foraminifer test precipitation rate (as discussed in Section 5.2). The $\delta^{44}Ca$ of the cultured foraminifera shows a positive dependence on DIC ($R^2 = 0.5$, $p = 0.13$), but a more significant correlation with $[CO_3^{2-}]$ ($R^2 = 0.86$, $p = 0.031$) (Fig. 3h–i). No significant correlation is observed between $\delta^{44}Ca$ and pH (Fig. 3g).

4.2. Core-top study

To avoid large uncertainties arising from GLODAP-derived site-specific carbonate chemistry, we determined *in-situ* pH using $\delta^{11}B$ on the same foraminifer samples. This parallel determination of $\delta^{11}B$ with $\delta^{7}Li$ and Li/Ca from the same exact sample enabled us to produce a systematic record of the pH in which the foraminifer calcified. However, it should be noted that uncertainty in the $\delta^{11}B_{sw}$, particularly in porewaters, can potentially compromise the boron isotope-based pH reconstruction. For clarity, we show $\delta^{7}Li$ plotted against pH-derived from both $\delta^{11}B$ and GLODAP.

Similar to the culture study, a negative correlation between $\delta^{7}Li_{SHELL}$ and GLODAP-derived pH is observed in the core-top specimens of the species *C. mundulus* (Fig. 4A; $R^2 = 0.56$, $p = 0.006$), although this correlation is much weaker for *C. wuellerstorfi* ($R^2 = 0.20$, $p = 0.7$). A negative correlation between $\delta^{7}Li_{SHELL}$ and seawater pH derived from $\delta^{11}B_{SHELL}$ (Fig. 4B) is also observed for both the species of epi-benthic foraminifera, *C.wuellerstorfi* ($R^2 = 0.5$, $p = 0.5$) and *C. mundulus* ($R^2 = 0.76$, $p = 0.005$).

The $\delta^{7}Li$ of *C. wuellerstorfi* is only weakly correlated with GLODAP-derived concentrations of DIC ($R^2 = 0.23$, $p = 0.6$), whereas there is a significant positive correlation ($R^2 = 0.50$, $p = 0.02$) between *C. mundulus* and

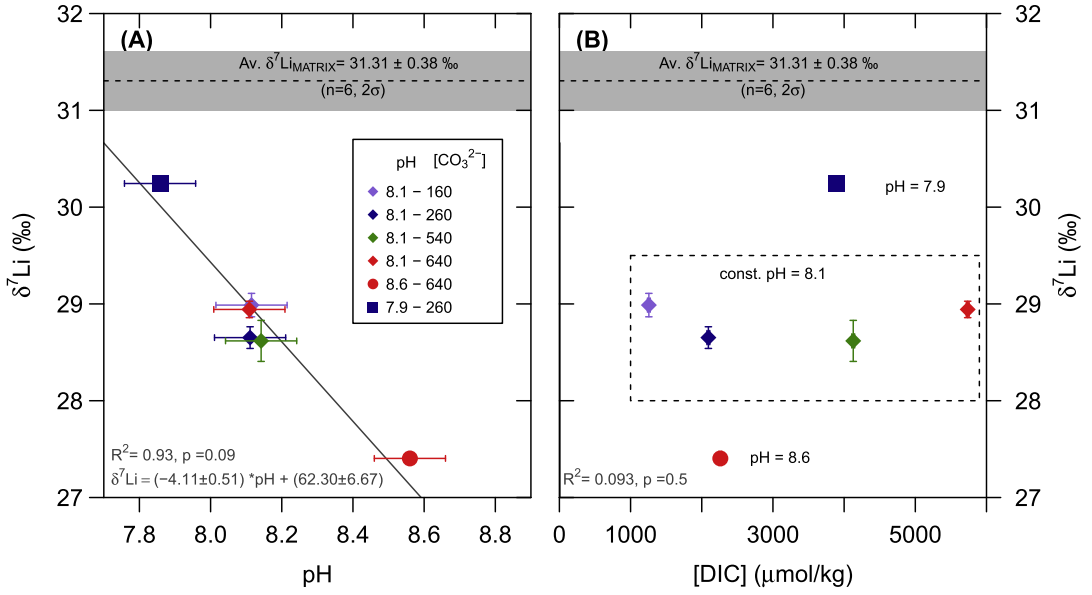

Fig. 2. The pH and DIC dependence of lithium isotopic composition (δ^7Li_{SHELL}) of cultured *A. lessonii*. See legend for pH and $[CO_3^{2-}]$ (µmol/kg) conditions of each treatment. The 2σ error of pH and [DIC] based on replicate measurements of the culture matrix was 0.1 pH units and 20 µmol/kg, respectively. The grey bar represents the 2σ external uncertainty of δ^7Li_{MATRIX} based on triplicate measurements.

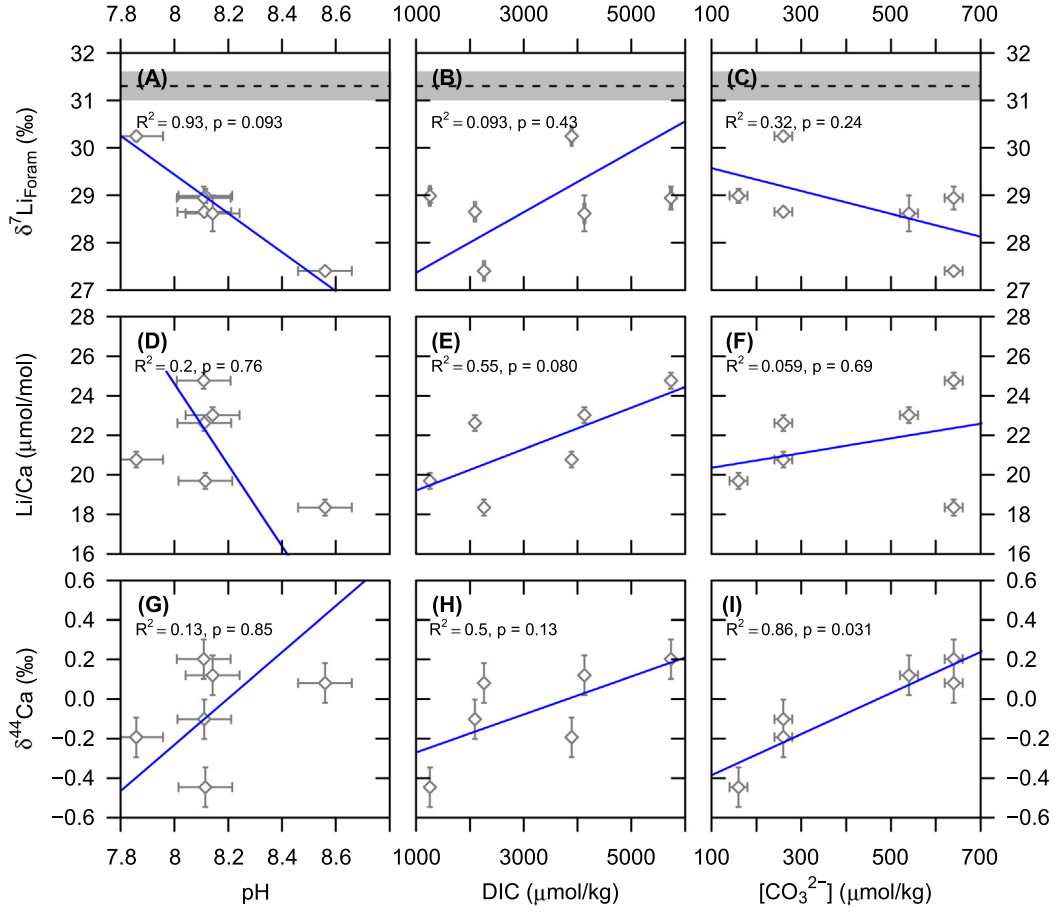

Fig. 3. Cultured *A. lessonii* δ^7Li, Li/Ca and $\delta^{44}Ca$ as a function of pH (left panel), DIC (centre panel) and $[CO_3^{2-}]$ (right panel). Black dashed line and grey horizontal bar show mean and 2σ external uncertainty of δ^7Li_{MATRIX} based on triplicate measurements.

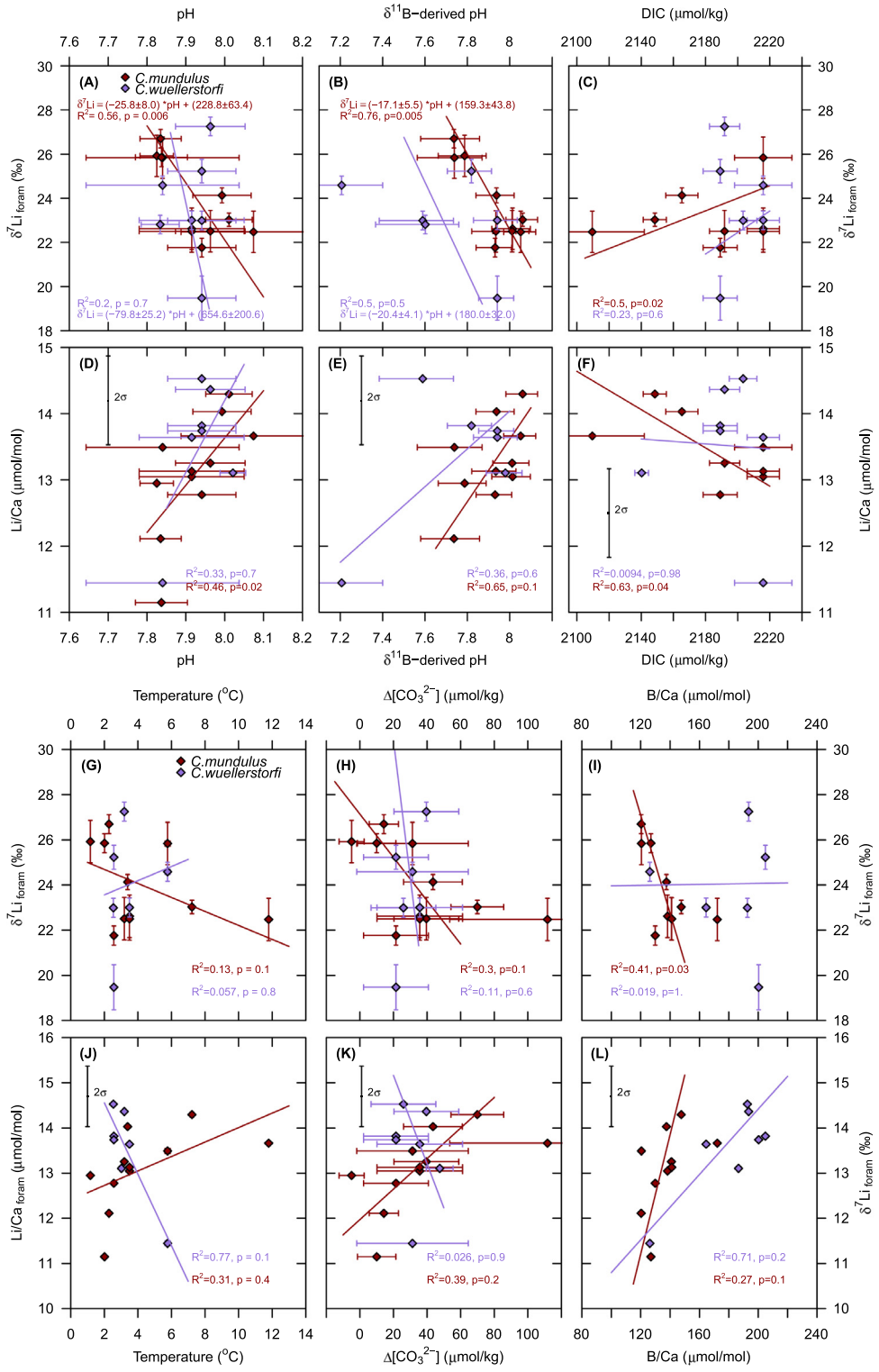

Fig. 4. Coretop *C. mundulus* (red) and *C. wuellerstorfi* (purple) δ^7Li (top), Li/Ca (bottom) relative to GLODAP-interpolated bottom water pH (A, D), foraminiferal δ^{11}B-derived pH (B, E), GLODAP-interpolated DIC (C, F), GLODAP-interpolated bottom water temperature (G, J), GLODAP-interpolated bottom water $\Delta[CO_3^{2-}]$ (H, K) and B/Ca (I, L). Analytical uncertainty (2σ) is based on replicate measurements of the sample (where available) or on replicate measurements of the NEP coral. (For interpretation of the references to colour in this figure legend, the reader is referred to the web version of this article.)

DIC concentration (Fig. 4C). As the concentration of DIC and pH are anti-correlated across the world ocean, a positive correlation between δ^7Li and the concentration of DIC is not unsurprising if δ^7Li is pH-dependent, as observed in the culture experiments.

The Li/Ca ratios of *C. mundulus* and *C. wuellerstorfi* are weakly positively correlated with pH (Fig. 4D, E), and weakly negatively correlated with DIC concentration (Fig. 4F). Li/Ca in *C.mundulus* shows a weak positive dependence on temperature and $\Delta[CO_3^{2-}]$, whereas *C. wuellerstorfi* is negatively correlated with bottom water temperature and not dependent on $\Delta[CO_3^{2-}]$ (Fig. 4J, K). However, given that the negative Li/Ca-T relationship for *C. wuellerstorfi* is driven by one data point, we would question the robustness of the apparent dependence. Furthermore, the comparison between *C. wuellerstorfi* B/Ca and Li/Ca (Fig. 4L) suggests a positive correlation between $\Delta[CO_3^{2-}]$ and Li/Ca.

4.3. Downcore study

Lithium and boron isotopic composition of the epibenthic species *C. mundulus* were determined on samples from core PS75/056-1 from the deep South Pacific (Fig. 5) spanning the last deglaciation at a temporal resolution of ≤2000 yrs. Note that where repeat samples have been obtained, there is some heterogeneity observed (e.g. at 14 ka). These repeat samples were not homogenised after crushing and therefore the isotopic difference likely reflects real isotopic heterogeneity amongst foraminifera from the same depth level, which may be a product of strong bioturbation (see Fig. S4).

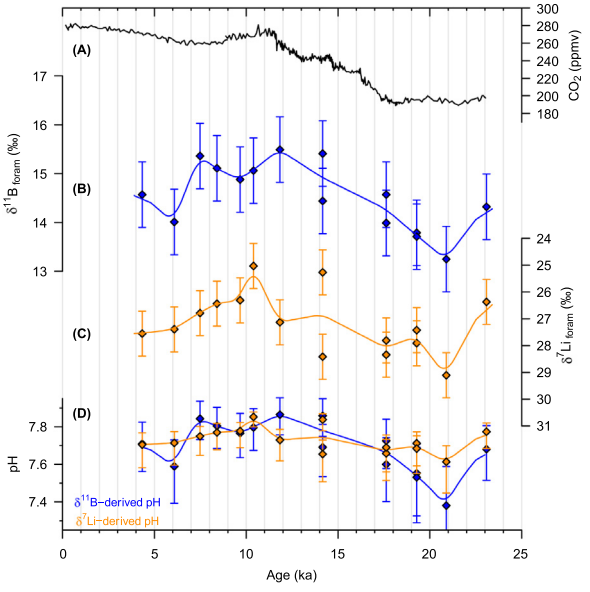

Fig. 5. Deglacial δ^{11}B and δ^7Li records from the deep South Pacific sediment core PS75/056–1. (A) Atmospheric pCO_2 (Monnin et al., 2004; Marcott et al., 2014); Deglacial *C. mundulus* (B) δ^{11}B and (C) δ^7Li record from PS75/056-1 (Note the reversed y-axis); (D) δ^{11}B- and δ^7Li-derived pH, blue and orange curves respectively. Analytical uncertainty (2σ) is based on homogenised replicate measurements of the sample (where available) or on replicate measurements of the NEP coral. (For interpretation of the references to colour in this figure legend, the reader is referred to the web version of this article.)

Despite possible distortion of the core by bioturbation, broad trends can still be observed. Foraminiferal δ^{11}B (Fig. 5b) is at a minimum during the last glacial maximum (LGM; 21–19 ka) and steadily increases across the last deglaciation to a maximum during the Pre-Boreal (12–10 ka). Similar to δ^{11}B, the record of δ^7Li (Fig. 5c) has a maximum (i.e. a pH minimum) during the LGM (note the reversed y-axis), and steadily decreases across the deglaciation to a minimum (i.e. pH maximum) at 10 ka. A discussion of the conversion of δ^{11}B and δ^7Li to pH can be found in Section 5.4.

5. DISCUSSION

The key results from the present study are, (i) δ^7Li of cultured *A. lessonii* is strongly dependent on the pH of the growth matrix (Fig. 2a), and there is no dependence of δ^7Li on DIC (Fig. 2b), and (ii) globally-distributed core-top *C. wuellerstorfi* and *C. mundulus* δ^7Li demonstrate a similar pH-dependence, albeit with a higher degree of scatter. Additionally, a strong negative correlation between δ^7Li and δ^{11}B observed in all samples (Fig. 6).

In the following, we discuss in detail the δ^7Li and Li/Ca results of our culture and core-top study relative to other published foraminiferal lithium studies (Section 5.1). We then discuss possible inorganic and biological controls on lithium incorporation into foraminifer calcite (Section 5.2), and produce a best-estimate for the δ^7Li sensitivity to pH (Section 5.3). Finally, we apply this calibration to a deglacial δ^7Li record from the South Pacific, making a comparison of the pH estimated based on δ^7Li and δ^{11}B (Section 5.4).

5.1. Culture study comparison

The δ^7Li and Li/Ca results from the present culture study are in contrast with the culture study of Vigier et al. (2015) who observed that δ^7Li was insensitive to changes in pH, but was positively correlated with DIC. Furthermore, Vigier et al. (2015) reported that Li/Ca ratios negatively correlate with DIC – opposite to our results. Since species of the same genus as Vigier et al. (2015) were investigated in the present study, it is unlikely that the observed discrepancy between the two studies is due to differences in the biomineralisation mechanism. We note that there are several shortfalls in the experimental set-up of Vigier et al. (2015), for example, seawater was boiled to remove dissolved CO_2; boiling can lead not only to uncontrolled precipitation but can also denaturate dissolved organic substances that are capable of significantly altering the bioavailability of essential trace elements and element speciation. Additionally, the δ^7Li and Li/Ca of the culture matrices were not reported. Vigier et al. (2015) reported foraminiferal δ^7Li ~10‰ higher than seawater for specimens cultured at high concentrations of DIC. This observation is in contrast to carbonate precipitation experiments that

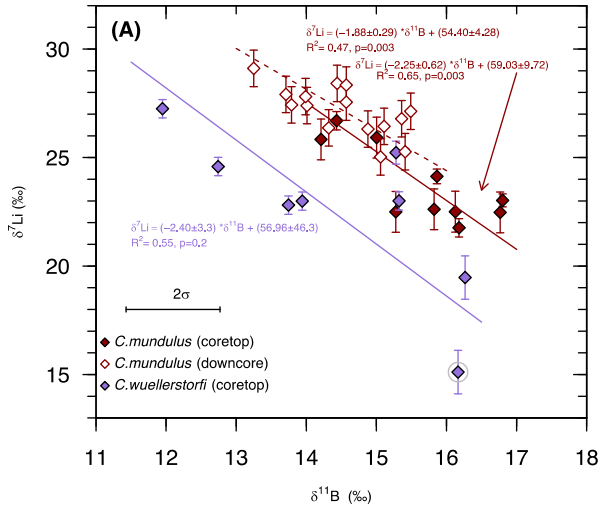

Fig. 6. Comparison between δ^7Li and δ^{11}B in core-top (closed symbols) and downcore (open symbols; PS75-056) *C. wuellerstorfi* (purple) and *C. mundulus* (red). Analytical uncertainty (2σ) is based on homogenised replicate measurements of the sample (where available) or on replicate measurements of the NEP coral. Outliers (residuals > 5σ) are highlighted by a grey circle and not included in the final regression. (For interpretation of the references to colour in this figure legend, the reader is referred to the web version of this article.)

unanimously suggest that δ^7Li of the precipitated carbonate is isotopically lower than seawater (Marriott et al., 2004a; Marriott et al., 2004b). Similarly, none of the published δ^7Li of foraminifera are isotopically higher than seawater (Hathorne and James, 2006; Misra and Froelich, 2012). We would therefore question whether the δ^7Li of the culture matrix was 31‰. Whilst there are clear limitations in the study of Vigier et al., (2015), these are not sufficient to explain the apparently opposite results that we see. We cannot offer a good explanation for why this is the case, suffice to say that further culture studies are required. However, we note that the strong and statistically significant negative correlation that we observe in our core-top study between δ^7Li and δ^{11}B-derived pH (Fig. 4B) suggests that pH is the dominant control over δ^7Li, as opposed to DIC (Fig. 4C).

5.2. Controls on the incorporation of lithium in foraminifer calcite

The present culture experiments demonstrate that the fractionation of lithium isotopes in foraminifer calcite is strongly dependent on pH but not on the concentration of DIC. However, the concentration of DIC appears to affect the Li/Ca ratio of foraminifer calcite. We discuss here the inorganic controls on lithium isotope fractionation that could account for the trends observed in the culture study.

The aqueous speciation of lithium is poorly understood (Richens, 1997; Winter and Andrew, 2000). In solution, the Li^+ ion exists as an aqueous ion (Loeffler et al., 2003). The number of water ligands (H_2O and/or OH^-) coordinating the Li^+ ion can range from 4 to 7 (Koneshan et al., 1998; Jahn and Wunder, 2009; Harsányi et al., 2012). A molecular dynamic simulation study by Hofmann et al., 2012 predicts that desolvation rates of Li^+ (and other alkali elements) may be strongly dependent on the metal cation mass. The mass difference between the two isotopes of lithium (^{6}Li and ^{7}Li) is ~17%. In nature, ^{6}Li is preferentially desolvated over ^{7}Li and enters the solid phase. This implies that there would be a large isotope fractionation associated with lithium incorporation into solid phase from solution (~25‰ as per Hofmann et al., 2012). Thus, authigenic clay minerals and precipitated calcite are both isotopically lower than the source fluid (Chan and Kastner, 2000; Marriott et al., 2004b), although the degree of isotope fractionation during clay precipitation ($\delta^7Li_{Fluid} - \delta^7Li_{Clay} = \Delta_{Fluid-Clay}$ ~18‰) is much larger than during calcite formation ($\delta^7Li_{Fluid} - \delta^7Li_{Calcite} = \Delta_{Fluid-Calcite}$ ~9‰) from seawater. We propose that any physio-chemical parameter that influences the hydration sphere of Li^+ would in turn impact the isotope fractionation associated with lithium incorporation into the solid phase from a solution ($\Delta_{Fluid-Solid}$).

Temperature, pressure, and pH should be the primary controls on the Li^+ hydration sphere provided the ionic strength of the solution remains constant (as is the case with seawater). Possibly the pH dependent change in Li^+ hydration is restricted to the second hydration sphere (Koneshan et al., 1998) in the range of pH of the present study. Ab-initio calculations of lithium isotope fractionation associated with $CaCO_3$ precipitation by Bogatko et al., 2013 predicts strong temperature dependence and no pH effect within the pH range of seawater. However, experimental work by Marriott et al., 2004a, 2004b has demonstrated that lithium isotope fractionation during calcite precipitation is minimally temperature dependent within 5 °C and 25 °C, i.e. 0.03 ± 0.04‰ per degree C. Note the large uncertainty associated with the calculated sensitivity. Moreover, below 90 °C the $\Delta_{Fluid-Clay}$ is also insensitive to the temperature of precipitation (Vigier et al., 2008). Note that the pH dependency of $\Delta_{Fluid-Clay}$ remains uninvestigated. Since all foraminifer specimens in this study were cultured at constant temperature and since the temperature dependence of lithium isotopic composition in calcite (0.03 ± 0.04‰ per degree C) is analytically unresolvable across a temperature range of few tens of degree C (external analytical precision of δ^7Li determination is ±0.5‰), we consider the temperature effect to be unimportant in this study.

We hypothesise that the change in hydroxyl ion concentration [OH^-] with pH alters the hydration sphere of the Li^+ ion in solution and thus influences the lithium isotope fractionation associated with lithium desolvation. At high pH, a larger hydration sphere and/or increased Li^+–OH^- coordination would, in principle, imply a greater difference in the desolvation energy of ^{6}Li and ^{7}Li and thus a larger $\Delta_{Fluid-Calcite}$ and possibly a lower Li/Ca in calcite.

In the culture experiments, Li/Ca is not dependent on pH, but rather shows a dependency on DIC. Could there be a second inorganic process controlling Li/Ca in foraminifera? Inorganic precipitation experiments have suggested that at a faster rate of crystal growth, the concentration

of alkali metals in calcite may increase as a result of a greater incorporation of alkali metals into interstitial positions within the crystal structure (Okumura and Kitano, 1986). In biological systems, determination of the crystal growth rate is difficult. Individual shells tend to be heavier in higher [CO_3^{2-}] growth environments (Bijma et al., 1999; Henehan et al., 2017), but it cannot be categorically concluded that this weight change is due to an increase in the precipitation rate. In the literature, crystal growth rate is often assumed to be equivalent to shell growth rate; however, we stress that these two concepts are not the same. However, making the assumption that shell growth rate and crystal growth rate are at least positively correlated, it is possible to look at the effect of variations in growth rate on Li/Ca. In this study, foraminifera were grown under variable [CO_3^{2-}] conditions, and therefore we could use our experiments to test whether [CO_3^{2-}] has an effect on shell growth rate and thus on shell Li/Ca. Unfortunately, the estimates of shell growth rate in Kaczmarek et al. (2015) are not accurate because average shell growth rates were determined using the final shell weight divided by the number of days in the culture, rather than measuring the shell size weekly. This is an important oversight as the cultured foraminifera were sometimes dead before they were removed from the culture, and so the "dead time" is not factored into the growth rate estimates in Kaczmarek et al. (2015). However, it may be possible to use $\delta^{44}Ca$ as a proxy for precipitation rate; it has been shown in multiple studies of inorganic calcite and aragonite precipitation there is increased calcium isotope fractionation at higher precipitation rates, producing ^{40}Ca enriched carbonate minerals (Gussone et al., 2003; Tang et al., 2008; DePaolo, 2011). It is unclear whether the same change in calcium isotope fractionation factor with changing growth rate occurs during biomineralisation, and it may be difficult to deconvolve the effect of temperature and precipitation rate due to the small changes in the calcium isotope fractionation each produces. We observe a strong positive correlation between [CO_3^{2-}] and $\delta^{44}Ca_{SHELL}$ ($R^2 = 0.86$; Fig. 3i). Similarly, Kisakürek et al. (2011) observe a decrease in calcium isotope fractionation in foraminifera cultured in media at constant temperature with increasing pH. From first principles, it would be expected that at higher [CO_3^{2-}], the biomineral precipitation rate would be higher, which in the inorganic studies leads to carbonate with a lower $\delta^{44}Ca$ (Tang et al., 2008; DePaolo, 2011). The positive correlation between [CO_3^{2-}] and $\delta^{44}Ca$ observed in this study and the Kisakürek et al. (2011) culture study suggests foraminifera behave fundamentally different to inorganic systems and that with an increase in the growth rate of the foraminifera there is a decrease in the calcium isotopic fractionation observed. Whilst we emphasise the uncertainty in assuming that foraminiferal $\delta^{44}Ca$ equates to growth rate, we note that there is no significant correlation between *A. lessonii* $\delta^{44}Ca$ and Li/Ca (Fig. S6, $R2 = 0.25$, $p = 0.55$), tentatively suggesting that growth rate has no effect on Li/Ca. More robust evidence that growth rate has no effect on Li/Ca comes from Langer et al., (2015). The shell growth rate of *A. lessonii* has been demonstrated to increase with [Ca] (Mewes et al., 2015), however, no effect on *A. lessonii* Li/Ca was observed in culture experiments in which the [Ca] of seawater was varied (Langer et al., 2015). This suggests that shell growth rate does not control Li/Ca. Note that crystal precipitation rate still might control Li/Ca, because it is unknown whether shell growth rate and crystal precipitation rate are correlated. A final piece of evidence arguing against a growth rate dependence of Li/Ca, is that there is no consistent relationship between the lithium concentration in our *A. lessonii* samples and the concentration of alkali metals (Na) or alkaline elements (e.g. Mg, Sr, Ba) (Fig. S7) unlike inorganically precipitated calcite (Okumura and Kitano, 1986; Marriott et al., 2004a, 2004b). Based on the above lines of evidence, we suggest that lithium incorporation into biogenic calcite is independent of growth rate.

The above discussion highlights a number of problems with an inorganic explanation for the δ^7Li and Li/Ca observed in our *A. lessonii* samples; (i) the $\Delta_{Fluid-Calcite}$ observed in *A. lessonii* is much smaller (1–3‰) than the $\Delta_{Fluid-Calcite}$ expected based on inorganic precipitation experiments (~9‰), (ii) there is no observed trend between *A. lessonii* Li/Ca and pH as might be expected based on the isotopic fractionation, and (iii) variations in shell growth rate cannot explain the Li/Ca ratios observed. Therefore, we briefly try to explain the data within the framework of existing biomineralisation models.

It has been long since noticed that foraminifera exert a tight control on chamber formation. Although extracellular, chamber formation takes place inside a so-called delimited biomineralization space (DBS, Erez, 2003). The DBS pH is elevated (ca. pH 9) to facilitate calcite precipitation (Bentov et al., 2009; de Nooijer et al., 2009). It is unknown whether DBS pH changes with seawater pH; however, given the strong dependency of foraminiferal δ^7Li on pH, there is some indication that DBS pH likely depends on seawater pH. We suggest that the same ideas of a pH dependency of the lithium hydration sphere can be applied to the pH of the DBS, although we acknowledge that we currently have no way of determining whether fractionation occurs at the mineral growth surface or during the transport of Li across biological membranes during biomineralisation.

Based on our culture experiments, the concentration of DIC appears to exert a first order control on Li/Ca (Fig. 3e; $R^2 = 0.55$, $p = 0.08$). How does this mechanism work? Transmembrane transport of ions from seawater into the DBS has been used to account for the positive correlation of Sr/Ca in *Ammonia sp.* and seawater DIC concentration (Keul et al., 2017). It is tempting to apply this explanation to the positive relationship between Li/Ca and DIC in *Amphistegina* (Fig. 3e). This, however, is not possible because the explanation in Keul et al. (2017) assumes a competition between Ca and the minor element. Alkali metal ions such as Li do not compete with Ca and their behaviour, therefore, requires another model. Langer et al. (2015) focuses on a Ca-channel mediated Li transport across the plasma-membrane. Since foraminifera have a high requirement for DIC during chamber formation, they probably employ HCO_3^- transporters to meet this requirement (Keul et al., 2017). A HCO_3^-/Na co-

transporter, with Li readily substituting for Na (Jentsch et al., 1984) is a likely candidate. Under high seawater DIC (and therefore HCO_3^-) concentrations, more HCO_3^- (Keul et al., 2017) and therefore more Li relative to Ca is transported into the DBS, increasing the foraminiferal Li/Ca ratio. This scenario predicts that Na, like Li, should display a positive correlation with seawater [HCO_3^-]. But this is not the case in the cultured *A. lessonii* (Fig. S7a; $R^2 = 0.06$, $p = 0.79$). Potentially there is a second Na transporter that can account for the decoupling between Na and Li, however further culturing experiments that target trace elements (in particular other alkali metals) will be required to understand the nuances of lithium incorporation in foraminifera.

In summary, the culture data suggests that the incorporation of lithium into foraminiferal calcite appears to be dependent on external carbon chemistry. We suggest that pH-dependent changes in the hydration sphere of lithium could produce isotope fractionation either at the mineral growth surface or during the transport of Li across biological membranes during biomineralisation leading to the observed pH-δ^7Li relationship. Additionally, there appears to be a dependency of Li/Ca on DIC concentration which does not have an associated isotopic fractionation; however, the exact transport pathway remains enigmatic. It is perhaps surprising that whilst the core-top data supports our understanding of the pH-dependence of δ^7Li, core-top *C. mundulus* data suggests the opposite relationship between Li/Ca and DIC (Fig. 4F) than the culture data. We emphasise that the unlike the culture study, the core-top sites do not represent a designed experimental setup, and therefore a correlation between two variables does not necessary imply causation. It is therefore possible that some secondary variable that actually controls Li/Ca, which was not investigated by the culture experiments (e.g. temperature or salinity), may be inversely correlated with DIC concentration in the global ocean, and may result in an apparent negative trend between Li/Ca and DIC concentration. Temperature, for example, is a good candidate for such a variable. At deeper depths within the global ocean, there is often a higher DIC concentration and lower temperature. Indeed, several studies have observed the benthic foraminifera Li/Ca is negatively correlated with temperature (Hall and Chan, 2004; Marriott et al., 2004b; Bryan and Marchitto, 2008), whilst others have suggested that benthic foraminifera Li/Ca is positively correlated with $\Delta[CO_3^{2-}]$ (Lear and Rosenthal, 2006). Note that this is just an example and we are not advocating that temperature is a control on Li/Ca, merely that it (or another unknown variable) can be used to explain seeming inconsistencies between culture and core-top Li/Ca. In order to definitively determine the controls on foraminifera Li/Ca, further culture experiments testing a greater number of variables will be required. We can conclude that whilst DIC concentration appears to exert a secondary control Li/Ca, there is likely a primary (and as yet unknown) control on Li/Ca present in the real ocean. However, we can rule out $\Delta[CO_3^{2-}]$ and pH based on our culture experiments.

5.3. δ^7Li-pH calibration

Utilising the culture and core-top results, an empirical sensitivity of δ^7Li to pH is determined. The cultured *A. lessonii* have a δ^7Li-pH sensitivity of -4.11 ± 0.51‰/pH unit (Fig. 2a). By contrast, the core-top *C. mundulus* and *C. wuellerstorfi* specimens indicate a higher sensitivity of -25.8 ± 8.0 and -79.8 ± 25.0‰/pH unit, respectively. There are a number of possible reasons for this difference; (i) uncertainty in the GLODAP-inferred pH estimates, (ii) the requirement for species-specific calibration curves, or (iii) non-linearity of the δ^7Li-pH sensitivity over a large pH range. As discussed earlier, the GLODAP-inferred bottom water pH estimates could be significantly different to the actual pH conditions experienced by the benthic foraminifera. The δ^7Li-pH sensitivity (where pH has been instead derived from δ^{11}B) is -17.1 ± 5.5 and -20.4 ± 4.1‰/pH unit for *C. mundulus* and *C. wuellerstorfi* respectively. Though the sensitivity is significantly lower, these boron-derived sensitivities are still more than double that of the culture δ^7Li-pH sensitivity. This might suggest that the δ^7Li dependence on pH is species-specific, or this can be a result of non-linearity in the δ^7Li-pH curve. The low pH resolution of the culture study (3 experiments spanning a pH range of 7.9–8.6) could have failed to capture the potentially non-linear and thus higher δ^7Li-pH sensitivity over the narrower pH range of 7.8–8.1 as recorded in the core-top study. Strategic culture studies are required to discern between the two hypotheses.

We emphasise that although the absolute uncertainties in the δ^{11}B-derived pH-δ^7Li sensitivity are smaller than for the GLODAP-inferred pH-δ^7Li sensitivity, the percentage error in the sensitivity is still large; 30% for *C. mundulus* and 30% for *C. wuellerstorfi*. More culture and core-top studies (with *in-situ* carbonate chemistry) are required to better constrain the δ^7Li-pH sensitivity before δ^7Li can be used as an independent proxy to determine past ocean pH.

Whilst we acknowledge that this is a pilot study and further work in the δ^7Li-pH proxy development is required, we suggest that foraminiferal δ^7Li could make a good compliment to δ^{11}B when determining pH in the past. As the δ^7Li-pH sensitivity is of the opposite sense to the δ^{11}B-pH relationship (Fig. 6), it is theoretically possible to use both δ^7Li and δ^{11}B in conjunction to improve the confidence of seawater pH reconstructions. Whilst there is a strong temperature dependency of boron isotopic fractionation, evidence from inorganic calcite precipitation studies (Marriott et al., 2004a, 2004b) and culture studies (Vigier et al., 2015) suggests that temperature may be less important in driving lithium isotope fractionation. Therefore, in situations where paleo-temperature reconstructions limit the accuracy to which the dissociation constant of boron (K_B) can be determined (affecting the accuracy of δ^{11}B-derived pH reconstructions), foraminiferal δ^7Li might be used as a secondary independent pH proxy. However, we emphasise that before this can be applied more widely to paleo-records, further culture and inorganic precipitation experiments are required to determine other secondary controls on foraminiferal δ^7Li.

An intriguing observation is that the isotopic composition of lithium and boron appears to follow mass dependent fractionation (Δm/M). The core-top δ^7Li-δ^{11}B curves (Fig. 6) have sensitivities of 1.88 and 2.25‰/‰ for *C. mundulus* and *C. wuellerstorfi* respectively. This is broadly consistent with the relative mass difference of the two isotopes lithium (^{6}Li and ^{7}Li; $\Delta m_{7Li-6Li} = 1.001$; $M_{6Li} = 6.015$; $\Delta m_{7Li-6Li}/M_{6Li} = 0.1664$) and that of boron (^{10}B and ^{11}B; $\Delta m_{11B-10B} = 0.9964$; $M_{10B} = 10.013$; $\Delta m_{11B-10B}/M_{10B} = 0.0995$) of 1.67. Although the determining mechanism controlling isotopic fraction of boron and lithium are different – i.e. boron isotopic fractionation is controlled by the speciation of dissolved boron in seawater, whereas lithium isotopic fractionation is hypothesised to be controlled by differences in the desolvation energy of ^{6}Li and ^{7}Li ions – from the observation that isotopic composition of lithium and boron appears to follow mass dependent fractionation. We therefore suggest that inorganic processes ultimately control the incorporation both lithium and boron into biogenic calcite.

5.4. Reconstructing paleo-pH: δ^7Li and δ^{11}B comparison

We use the lithium and boron isotopic composition recorded in *C. mundulus* from core PS75/056-1 from the deep South Pacific (Fig. 1) to reconstruct pH over the last deglaciation (Fig. 5). The δ^{11}B based pH determination suggest a pH minimum during the last glacial maximum (LGM). In contrast, the large 2σ uncertainty in the δ^7Li-pH calibration means that a similar pH minimum cannot be identified outside of analytical uncertainty. A pH minimum in the deep South Pacific during the LGM is consistent with the idea that the deep ocean's respired carbon reservoir was enlarged during glacial periods (Siegenthaler and Sarmiento, 1993; Toggweiler, 1999). A complete discussion of the South Pacific glacial carbon reservoir, including a high-resolution δ^{11}B record from this site, is not the focus of the present manuscript and will be the subject of a future publication.

Of interest here is the quantitative conversion of the δ^7Li and δ^{11}B records to pH (Fig. 5d). Bottom water pH is calculated from δ^{11}B assuming (i) $\alpha_B = 1.0272$ (Klochko et al., 2006), (ii) $\delta^{11}B_{sw} = 39.61$‰ (Foster et al., 2010), (iii) $B_T = 432.5 \times (S/35)$ μmol/kg (Lee et al., 2010) and (iv) no fractionation between seawater borate and foraminifera calcite in *C. mundulus* (Rae et al., 2011). The dissociation constant for the reaction of boric acid to borate (pK_B^*) is a function of temperature, salinity and pressure (Dickson, 1990). As there are no direct temperature or salinity reconstructions from this site spanning the last deglaciation, we assume that temperatures monotonically increase from −1.2 °C (based on the Chatham Rise core ODP1123 (Adkins et al., 2002) to the present day bottom water temperature of 1.17 °C between 20–10 ka (Fig. S5a). Similarly, we assume that the bottom water salinity decreases by 1.5 psu (Adkins et al., 2002) across the same time period (Fig. S5b). Alternative temperature and salinity scenarios were tested (see Supporting Information; Fig. S5c), but the overall effect on pH is less than 0.03 pH units – a similar magnitude error to the replicate measurement based analytical uncertainty. Despite the uncertainties in the reconstruction of temperature and salinity, the δ^{11}B record suggest a pH increase of at least a 0.1 pH from the LGM to the Early Holocene (Fig. 5d).

We apply the core-top *C. mundulus* δ^{11}B-derived pH-δ^7Li calibration ($\delta^7Li = (-17.1 \pm 5.5)^* pH + (159.3 \pm 43.8)$; Fig. 4A) to derived pH from δ^7Li. We use this calibration, as opposed to the GLODAP pH-δ^7Li calibration, as the associated uncertainty is smaller. We acknowledge the use of this calibration means that δ^{11}B and δ^7Li are not fully decoupled, and thus we emphasise the need for a more robust core-top calibration in the future. However, based on this single calibration, the deglacial change in δ^7Li-derived pH is considerably damped compared to δ^{11}B-derived estimates (Fig. 5d).

The discrepancy between the δ^7Li- and δ^{11}B-derived pH in the South Pacific record can be caused by (i) uncertainties in the δ^7Li-pH regression, or (ii) downcore variations in porewater/seawater δ^{11}B that cannot be resolved. Propagated errors from the conversion of core-top δ^{11}B to pH result in large uncertainty in the δ^{11}B-derived pH-δ^7Li calibration, which will ultimately affect the accuracy of the downcore δ^7Li-derived pH estimates. It is therefore imperative that culture studies on *C. mundulus* or core-top studies with accurate carbonate chemistry are required to accurately determine the sensitivity of the *C. mundulus* δ^7Li-pH regression. However, it is possible to make the argument that the *C. mundulus* δ^7Li-derived pH record is correct, and that the δ^{11}B-derived pH is affected by variations in porewater/seawater δ^{11}B. Processes within the sediment column e.g. boron desorption from clays or sulphate reduction, can lead to porewaters that are isotopically light relative to seawater (e.g. Brumsack and Zuleger, 1992). It is possible that higher organic carbon fluxes during the glacial could have led to elevated rates of sulphate reduction, and thus a lower the porewater δ^{11}B (and consequently the foraminiferal δ^{11}B) than in the modern, producing pH estimates that are artificially low. Supporting evidence that the deep South Pacific may not have had a significantly lower pH during the LGM comes from reconstructions of deep Pacific carbonate chemistry (Yu et al., 2013), which shows no significant glacial-interglacial variability in the saturation state. However, it should be noted that B/Ca ratios from our downcore site are lower in the glacial period than in the Holocene (Supporting Material), and thus do not support the idea of boron desorption within the sediment column.

6. CONCLUSION

This study demonstrates that foraminiferal δ^7Li is strongly dependent on the pH of ambient seawater. This was established first in culture experiments on *A. lessonii* where the pH-CO_3^{2-} were decoupled. Furthermore, it was demonstrated that the δ^7Li-pH relationship holds true in a globally-distributed core-top study on the two commonly-used epi-benthic foraminifera *C. mundulus* and *C. wuellerstorfi.* A δ^7Li-pH calibration was established for each species; however, we emphasise that a lack of *in-situ* measurements of carbonate chemistry at these sites results

in significant uncertainties associated with each calibration. The *C. mundulus* δ^7Li-pH calibration is applied to a deglacial record from the deep South Pacific. We note that there are significant differences between the pH values derived from δ^7Li and δ^{11}B. Whilst this is likely an artefact of uncertainties in the δ^7Li-pH calibration, time-dependent variations in the δ^{11}B of the porewater could also contribute to the discrepancies. Further core-top (with in-situ carbonate chemistry) and culture studies are required to accurately determine the δ^7Li-pH sensitivity.

The major incentive behind establishing a δ^7Li-pH proxy to compliment δ^{11}B-based pH reconstructions, is that, unlike boron, there is no discernible dependence of lithium speciation on temperature. Therefore, uncertainty in δ^{11}B-derived pH reconstructions, from propagated error of uncertainty in paleo-temperature reconstructions may be reduced with the complimentary use of δ^7Li. We hypothesise that lithium incorporation into foraminiferal calcite is controlled by the strength of the hydration sphere of the Li^+ ion in solution, which we argue is pH-dependent. Further work is required to characterise the controlling processes on lithium uptake in foraminiferal calcite.

The dependence of foraminiferal δ^7Li on pH has significant implications for long timescale (millions of years) reconstructions of seawater δ^7Li (Hathorne and James, 2006; Misra and Froelich, 2012). Planktonic foraminiferal δ^7Li shows an overall increasing trend across the Cenozoic (Misra and Froelich, 2012). Across this time period, from the Palaeocene to the present day, there was a long-term decrease in atmospheric pCO_2 (Beerling and Royer, 2011 and references therein), implying a long-term increase in mean ocean pH. Given the negative correlation between δ^7Li and pH observed in this study, and assuming the same trend holds for planktonic foraminifera, this would imply that the seawater δ^7Li variations across the Cenozoic were even greater than originally inferred. Moreover, events such as the Mid-Miocene Climatic Optimum (at interval of elevated atmospheric pCO_2), which see a sharp decrease in foraminiferal δ^7Li, mask an even larger change in seawater δ^7Li. Further work is now required to investigate the processes responsible for such large and abrupt changes in seawater δ^7Li.

ACKNOWLEDGEMENTS

We thank the crew and scientific parties of the Polarstern, *RRS* Charles Darwin, *RRS* James Cook and Marion Dufresne for providing sample material. We are grateful to C. Waelbroeck for providing radiocarbon data and General A. Sadekov for early discussion. M. Greaves was instrumental in completing the analytical work. We would like to acknowledge the integral role of Prof. Henry (Harry) Elderfield in seeding the science and his financial support in this project.

APPENDIX A. SUPPLEMENTARY MATERIAL

Supplementary data associated with this article can be found, in the online version, at https://doi.org/10.1016/j.gca.2018.02.038.

REFERENCES

Adkins J. F., McIntyre K. and Schrag D. P. (2002) The salinity, temperature, and δ^{18}O of the glacial deep ocean. *Science* **298**, 1769–1773.

Barker S., Greaves M. and Elderfield H. (2003) A study of cleaning procedures used for foraminiferal Mg/Ca paleothermometry. *Geochem., Geophys. Geosyst.* **4**, 8407.

Beerling D. J. and Royer D. L. (2011) Convergent cenozoic CO_2 history. *Nat. Geosci.* **4**, 418–420.

Bentov S., Brownlee C. and Erez J. (2009) The role of seawater endocytosis in the biomineralization process in calcareous foraminifera. *Proc. Natl. Acad. Sci. USA* **106**, 21500–21504.

Bijma J., Spero H. J. and Lea D. W. (1999) Reassessing foraminiferal stable isotope geochemistry: impact of the oceanic carbonate system (experimental results). In *Use of Proxies in Paleoceanography*. Springer, Berlin, Heidelberg, pp. 489–512.

Bogatko S., Claeys P., De Proft F. and Geerlings P. (2013) Li^+ speciation and the use of ^{7}Li/^{6}Li isotope ratios for ancient climate monitoring. *Chem. Geol.* **357**, 1–7.

Bohlin M. S., Misra S., Lloyd N., Elderfield H. and Bickle M. J. (2018) High precision determination of lithium and magnesium isotopes utilising single column separation and MC-ICPMS. *Rapid Commun. Mass Spectrom.* **32**, 93–104.

Boyer, T.P., Antonov, J.I., Baranova, O.K., Coleman, C., Garcia, H.E., Grodsky, A., Johnson, D.R., Locarnini, R.A., Mishonov, A.V., O'Brien, T.D., Paver, C.R., Reagan, J.R., Seidov, D., Smolyar, I.V., Zweng, M.M., Brien, T.D.O., Paver, C.R., Reagan, J.R., Seidov, D., Smolyar, I.V., Zweng, M.M., Sullivan, K.D., 2013. WORLD OCEAN DATABASE 2013, NOAA Atlas NESDIS 72. Sydney Levitus, Ed.; Alexey Mishonoc, Tech. Ed. NOAA Atlas, p. 209.

Boyle E. A. and Keigwin L. D. (1985) Comparison of Atlantic and Pacific paleochemical records for the last 215,000 years: changes in deep ocean circulation and chemical inventories. *Earth Planet. Sci. Lett.* **76**, 135–150.

Brumsack H.-J. and Zuleger E. (1992) Boron and boron isotopes in pore waters from ODP Leg 127, Sea of Japan. *Earth Planet. Sci. Lett.* **113**, 427–433.

Bryan S. P. and Marchitto T. M. (2008) Mg/Ca-temperature proxy in benthic foraminifera: new calibrations from the Florida Straits and a hypothesis regarding Mg/Li. *Paleoceanography* **23**, PA2220.

Chan L. H. and Kastner M. (2000) Lithium isotopic compositions of pore fluids and sediments in the Costa Rica subduction zone: implications for fluid processes and sediment contribution to the arc volcanoes. *Earth Planet. Sci. Lett.* **183**, 275–290.

DePaolo D. J. (2011) Surface kinetic model for isotopic and trace element fractionation during precipitation of calcite from aqueous solutions. *Geochim. Cosmochim. Acta* **75**, 1039–1056.

Dickson A. G. (1990) Thermodynamics of the dissociation of boric acid in synthetic seawater from 273.15 to 318.15 K. *Deep Sea Res. Part A Oceanogr. Res. Pap.* **37**, 755–766.

Erez J. (2003) The source of ions for biomineralization in foraminifera and their implications for paleoceanographic proxies. *Rev. Mineral. Geochem.* **54**, 115–149.

Fantle M. S. and DePaolo D. J. (2005) Variations in the marine Ca cycle over the past 20 million years. *Earth Planet. Sci. Lett.* **237**, 102–117.

Flesch G. D., Anderson A. R. and Svec H. J. (1973) A secondary isotopic standard for ^{6}Li/^{7}Li determinations. *Int. J. Mass Spectrom. Ion Phys.* **12**, 265–272.

Fontanier C., Metzger E., Waelbroeck C., Mé Jouffrea, LeFloch N., Jorissen F., Etcheber H., Bichon S., Chabaud G., Poirier D., Grémare A. and Deflandre B. (2013) Live (Stained) benthic foraminifera off walvis Bay, Namibia: a deep-sea ecosystem

under the influence of bottom nepheloid layers. *J. Foraminifer. Res.* **43**, 55–71.

Foster G. L., Pogge von Strandmann P. A. E. and Rae J. W. B. (2010) Boron and magnesium isotopic composition of seawater. *Geochem. Geophys. Geosyst.* **11**.

Gaillardet J., Lemarchand D., Göpel C. and Manhès G. (2001) Evaporation and sublimation of boric acid: application for boron purification from organic rich solutions. *Geostand. Geoanalytical Res.* **25**, 67–75.

Gottschalk J., Vázquez Riveiros N., Waelbroeck C., Skinner L. C., Michel E., Duplessy J. C., Hodell D. and Mackensen A. (2016) Carbon isotope offsets between benthic foraminifer species of the genus *Cibicides (Cibicidoides)* in the glacial sub-Antarctic Atlantic. *Paleoceanography* **31**, 1583–1602.

Gussone N., Eisenhauer A., Heuser A., Dietzel M., Bock B., Böhm F., Spero H. J., Lea D. W., Bijma J. and Nägler T. F. (2003) Model for kinetic effects on calcium isotope fractionation (δ^{44}Ca) in inorganic aragonite and cultured planktonic foraminifera. *Geochim. Cosmochim. Acta* **67**, 1375–1382.

Hall J. M. and Chan L.-H. (2004) Li/Ca in multiple species of benthic and planktonic foraminifera: thermocline, latitudinal, and glacial-interglacial variation. *Geochim. Cosmochim. Acta* **68**, 529–545.

Harsányi I., Temleitner L., Beuneu B. and Pusztai L. (2012) Neutron and X-ray diffraction measurements on highly concentrated aqueous LiCl solutions. *J. Mol. Liq.* **165**, 94–100.

Hathorne E. C. and James R. H. (2006) Temporal record of lithium in seawater: a tracer for silicate weathering? *Earth Planet Sci. Lett.* **246**, 393–406.

Henehan M. J., Evans D., Shankle M., Burke J. E., Foster G. L., Anagnostou E., Chalk T. B., Stewart J. A., Alt C. H. S., Durrant J. and Hull P. M. (2017) Size-dependent response of foraminiferal calcification to seawater carbonate chemistry. *Biogeosciences* **14**, 3287–3308.

Hippler D., Eisenhauer A. and Nägler T. F. (2006) Tropical Atlantic SST history inferred from Ca isotope thermometry over the last 140ka. *Geochim. Cosmochim. Acta* **70**, 90–100.

Hofmann A. E., Bourg I. C. and DePaolo D. J. (2012) Ion desolvation as a mechanism for kinetic isotope fractionation in aqueous systems. *Proc. Natl. Acad. Sci. USA* **109**, 18689–18694.

Jahn S. and Wunder B. (2009) Lithium speciation in aqueous fluids at high P and T studied by ab initio molecular dynamics and consequences for Li-isotope fractionation between minerals and fluids. *Geochim. Cosmochim. Acta* **73**, 5428–5434.

Jentsch T. J., Keller S. K., Koch M. and Wiederholt M. (1984) Evidence for coupled transport of bicarbonate and sodium in cultured bovine corneal endothelial cells. *J. Membr. Biol.* **81**, 189–204.

Kaczmarek K., Langer G., Nehrke G., Horn I., Misra S., Janse M. and Bijma J. (2015) Boron incorporation in the foraminifer *Amphistegina lessonii* under a decoupled carbonate chemistry. *Biogeosciences* **12**, 1753–1763.

Keul N., Langer G., Thoms S., de Nooijer L. J., Reichart G.-J. and Bijma J. (2017) Exploring foraminiferal Sr/Ca as a new carbonate system proxy. *Geochim. Cosmochim. Acta* **202**, 374–386.

Key R. M., Kozyr A., Sabine C. L., Lee K., Wanninkhof R., Bullister J. L., Feely R. A., Millero F. J., Mordy C. and Peng T.-H. (2004) A global ocean carbon climatology: results from global data analysis project (GLODAP). *Global Biogeochem. Cycles* **18**, 1–23.

Kisakürek B., Eisenhauer A., Böhm F., Hathorne E. C. and Erez J. (2011) Controls on calcium isotope fractionation in cultured planktic foraminifera, *Globigerinoides ruber* and *Globigerinella siphonifera*. *Geochim. Cosmochim. Acta* **75**, 427–443.

Klochko K., Kaufman A. J., Yao W., Byrne R. H. and Tossell J. A. (2006) Experimental measurement of boron isotope fractionation in seawater. *Earth Planet. Sci. Lett.* **248**, 276–285.

Koneshan S., Rasaiah J. C., Lynden-Bell R. M. and Lee S. H. (1998) Solvent structure, dynamics, and ion mobility in aqueous solutions at 25 °C. *J. Phys. Chem. B* **102**, 4193–4204.

Langer G., Sadekov A., Thoms S., Mewes A., Nehrke G., Greaves M., Misra S., Bijma J. and Elderfield H. (2015) Li partitioning in the benthic foraminifera *Amphistegina lessonii*. *Geochemistry. Geophys. Geosyst.* **16**, 4275–4279.

Lear C. H. and Rosenthal Y. (2006) Benthic foraminiferal Li/Ca: insights into Cenozoic seawater carbonate saturation state. *Geology* **34**, 985–988.

Lee K., Kim T.-W., Byrne R. H., Millero F. J., Feely R. A. and Liu Y.-M. (2010) The universal ratio of boron to chlorinity for the North Pacific and North Atlantic oceans. *Geochim. Cosmochim. Acta* **74**, 1801–1811.

Lisiecki L. E. and Raymo M. E. (2005) A Pliocene-Pleistocene stack of 57 globally distributed benthic δ^{18}O records. *Paleoceanography* **20**.

Lloyd N. S., Sadekov A. Y. and Misra S. (2018) Application of 10^{13} ohm Faraday cup current amplifiers for boron isotopic analyses by solution mode and laser ablation MC-ICP-MS. *Rapid Commun. Mass Spectrom.* **32**, 9–18.

Loeffler H. H., Mohammed A. M., Inada Y. and Funahashi S. (2003) Lithium(I) ion hydration: a QM/MM-MD study. *Chem. Phys. Lett.* **379**, 452–457.

Marcott S. A., Bauska T. K., Buizert C., Steig E. J., Rosen J. L., Cuffey K. M., Fudge T. J., Severinghaus J. P., Ahn J., Kalk M. L., McConnell J. R., Sowers T., Taylor K. C., White J. W. C. and Brook E. J. (2014) Centennial-scale changes in the global carbon cycle during the last deglaciation. *Nature* **514**, 616–619.

Marriott C. S., Henderson G. M., Belshaw N. S. and Tudhope A. W. (2004a) Temperature dependence of δ^{7}Li, δ^{44}Ca and Li/Ca during growth of calcium carbonate. *Earth Planet. Sci. Lett.* **222**, 615–624.

Marriott C. S., Henderson G. M., Crompton R., Staubwasser M. and Shaw S. (2004b) Effect of mineralogy, salinity, and temperature on Li/Ca and Li isotope composition of calcium carbonate. *Chem. Geol.* **212**, 5–15.

Mewes A., Langer G., Thoms S., Nehrke G., Reichart G. J., De Nooijer L. J. and Bijma J. (2015) Impact of seawater [Ca^{2+}] on the calcification and calcite Mg/Ca of *Amphistegina lessonii*. *Biogeosciences* **12**, 2153–2162.

Millot R., Guerrot C. and Vigier N. (2004) Accurate and high-precision measurement of lithium isotopes in two reference materials by MC-ICP-MS. *Geostand. Geoanalytical Res.* **28**, 153–159.

Misra S. and Froelich P. N. (2012) Lithium isotope history of cenozoic seawater: changes in silicate weathering and reverse weathering. *Science* **335**, 818–823.

Misra S., Greaves M., Owen R., Kerr J., Elmore A. C. and Elderfield H. (2014a) Determination of B/Ca of natural carbonates by HR-ICP-MS.. *Geochem. Geophys. Geosystems* **15**, 1617–1628.

Misra S., Owen R., Kerr J., Greaves M. and Elderfield H. (2014b) Determination of δ^{11}B by HR-ICP-MS from mass limited samples: Application to natural carbonates and water samples. *Geochim. Cosmochim. Acta* **140**, 531–552.

Monnin E., Steig E. J., Siegenthaler U., Kawamura K., Schwander J., Stauffer B., Stocker T. F., Morse D. L., Barnola J.-M., Bellier B., Raynaud D. and Fischer H. (2004) Evidence for substantial accumulation rate variability in Antarctica during the Holocene, through synchronization of CO_2 in the Taylor Dome, Dome C and DML ice cores. *Earth Planet. Sci. Lett.* **224**, 45–54.

Nägler T. F., Eisenhauer A., Müller A., Hemleben C. and Kramers J. (2000) The δ^{44}Ca-temperature calibration on fossil and cultured *Globigerinoides sacculifer*: new tool for reconstruction of past sea surface temperatures. *Geochem. Geophys. Geosyst.* **1**, 1052.

de Nooijer L. J., Toyofuku T. and Kitazato H. (2009) Foraminifera promote calcification by elevating their intracellular pH. *Proc. Natl. Acad. Sci.* **106**, 15374–15378.

Okumura M. and Kitano Y. (1986) Coprecipitation of alkali metal ions with calcium carbonate. *Geochim. Cosmochim. Acta* **50**, 49–58.

Rae J. W. B., Foster G. L., Schmidt D. N. and Elliott T. (2011) Boron isotopes and B/Ca in benthic foraminifera: proxies for the deep ocean carbonate system. *Earth Planet. Sci. Lett.* **302**, 403–413.

Richens D. T. (1997) *The Chemistry of Aqua Ions : Synthesis, Structure, and Reactivity : A Tour Through the Periodic Table of the Elements, J*. Wiley.

Rosenthal Y., Boyle E. A. and Slowey N. (1997) Temperature control on the incorporation of magnesium, strontium, fluorine, and cadmium into benthic foraminiferal shells from Little Bahama Bank: prospects for thermocline paleoceanography. *Geochim. Cosmochim. Acta* **61**, 3633–3643.

Sabine C. L., Feely R. A., Gruber N., Key R. M., Lee K., Bullister J. L., Wanninkhof R., Wong C. S., Wallace D. W. R., Tilbrook B., Millero F. J., Peng T.-H., Kozyr A., Ono T. and Rios A. F. (2004) The oceanic sink for anthropogenic CO_2. *Science* **305**, 367–371.

Siegenthaler U. and Sarmiento J. L. (1993) Atmospheric carbon dioxide and the ocean. *Nature* **365**, 119–125.

Strelow F. W. E. (1984) Distribution coefficients and cation-exchange behaviour of 45 elements with a macroporous resin in hydrochloric acid/methanol mixtures. *Anal. Chim. Acta* **160**, 31–45.

Strelow F. W. E. (1989) Distribution coefficients and ion exchange behaviour of some chloride complex forming elements with bio rad Ag50W-Xb cation exchange resin in mixed nitric-hydrochloric acid solutions. *Solvent Extr. Ion Exch.* **7**, 735–747.

Tang J., Dietzel M., Böhm F., Köhler S. J. and Eisenhauer A. (2008) Sr^{2+}/Ca^{2+} and $^{44}Ca/^{40}Ca$ fractionation during inorganic calcite formation: II. Ca isotopes. *Geochim. Cosmochim. Acta* **72**, 3733–3745.

Toggweiler J. R. (1999) Variation of atmospheric CO_2 by ventilation of the ocean's deepest water. *Paleoceanography* **14**, 571–588.

Ullermann J., Lamy F., Ninnemann U., Lembke-Jene L., Gersonde R. and Tiedemann R. (2016) Pacific-atlantic circumpolar deep water coupling during the last 500 ka. *Paleoceanography*.

Vigier N., Decarreau A., Millot R., Carignan J., Petit S. and France-Lanord C. (2008) Quantifying Li isotope fractionation during smectite formation and implications for the Li cycle. *Geochim. Cosmochim. Acta* **72**, 780–792.

Vigier N., Rollion-Bard C., Levenson Y. and Erez J. (2015) Lithium isotopes in foraminifera shells as a novel proxy for the ocean dissolved inorganic carbon (DIC). *Comptes Rendus Geosci.* **347**, 43–51.

de Villiers S., Greaves M., Elderfield H., de Villiers S., Greaves M. and Elderfield H. (2002) An intensity ratio calibration method for the accurate determination of Mg/Ca and Sr/Ca of marine carbonates by ICP-AES. *Geochem. Geophys. Geosyst.* **3**, 1001.

Vogl J. and Rosner M. (2012) Production and certification of a unique set of isotope and delta reference materials for boron isotope determination in geochemical, environmental and industrial materials. *Geostand. Geoanalytical Res.* **36**, 161–175.

Wang B.-S., You C.-F., Huang K.-F., Wu S.-F., Aggarwal S. K., Chung C.-H. and Lin P.-Y. (2010) Direct separation of boron from Na- and Ca-rich matrices by sublimation for stable isotope measurement by MC-ICP-MS. *Talanta* **82**, 1378–1384.

Winter M. J. and Andrew J. E. (2000) *Foundations of Inorganic Chemistry*. Oxford University Press.

Yu J., Anderson R. F., Jin Z., Rae J. W. B., Opdyke B. N. and Eggins S. M. (2013) Responses of the deep ocean carbonate system to carbon reorganization during the Last Glacial–interglacial cycle. *Quat. Sci. Rev.* **76**, 39–52.

Associate editor: Thomas M. Marchitto